

Figure S1. MH[sim] is expressed at comparable levels to MH[mel] and does not phenocopy *mh* null. Related to Figure 1. (A) Western Blot of *mh[mel]* and *mh[sim]* ovaries probed with anti-FLAG and anti- α Tubulin. (B) Proportion of female progeny from *mh[mel]* and *mh[sim]* mothers. (C) Representative images of diploid embryos from crosses between *EGFP-cid* fathers and *mh[mel]* or *mh[sim]* mothers stained with anti-GFP. Diploid embryos are GFP-positive and haploid embryos are GFP-negative. (D) Ovary size estimates from *mh*¹ homozygous and *mh*¹/+ heterozygous females. (E) Number of mature eggs per ovary pair from *mh*¹ homozygous and *mh*¹/+ heterozygous females. (*t*-test: "n.s." $p > 0.05$, scale bar = 25 μm)

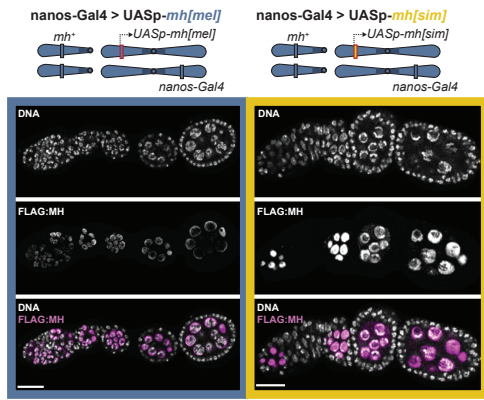
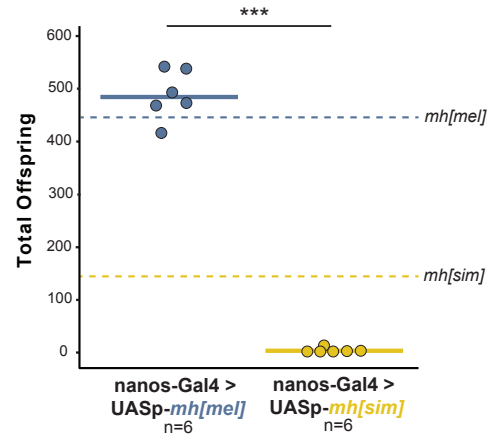
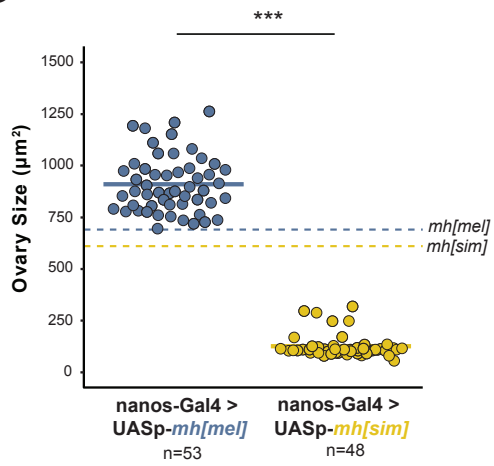
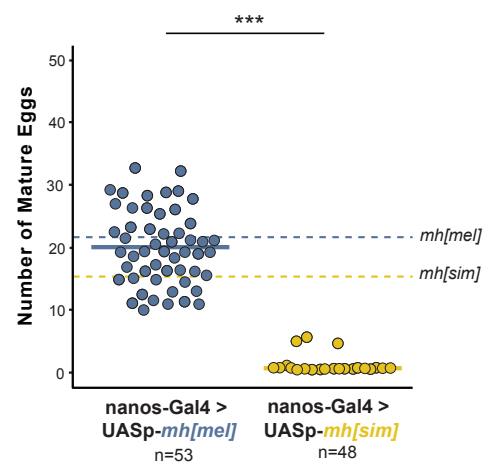
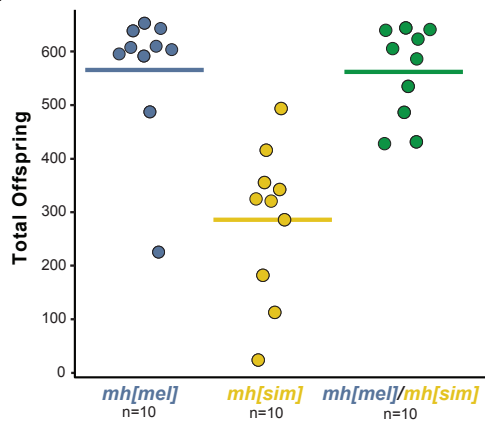
A**B****C****D****E**

Figure S2. MH[*sim*] toxicity is dose-dependent. Related to Figure 2. (A) Anti-FLAG staining of *mh[mel]* and *mh[sim]* upon overexpression under the UAS-GAL4 system. The driver nos-GAL4-VP16 expresses the *mh* transgene in the germline only. Corresponding chromosome X (wildtype) and chromosome 3 are shown in the images above. Note that wildtype *mh* is present in these genotypes. (B) Progeny counts of the nos-Gal4-VP16-driven UASp-*mh[mel]* or UASp-*mh[sim]* females crossed to wildtype (w^{1118}) males. (C) Ovary size estimates of the nos-Gal4-VP16-driven UASp-*mh[mel]* or UASp-*mh[sim]* females. (D) Number of mature eggs per ovary pair from nos-Gal4-VP16-driven UASp-*mh[mel]* or UASp-*mh[sim]* females. (E) Total offspring of *mh[mel]*, *mh[sim]*, and *mh[mel]/mh[sim]* heterozygous females crossed to wildtype (w^{1118}) males. In panels B, C, and D, dotted lines correspond to *mh[mel]* and *mh[sim]* averages reported in Figure 1C, 1E, and 1F, respectively. (*t*-test: “****” = $p < 0.001$, scale bar = 25 μ m)

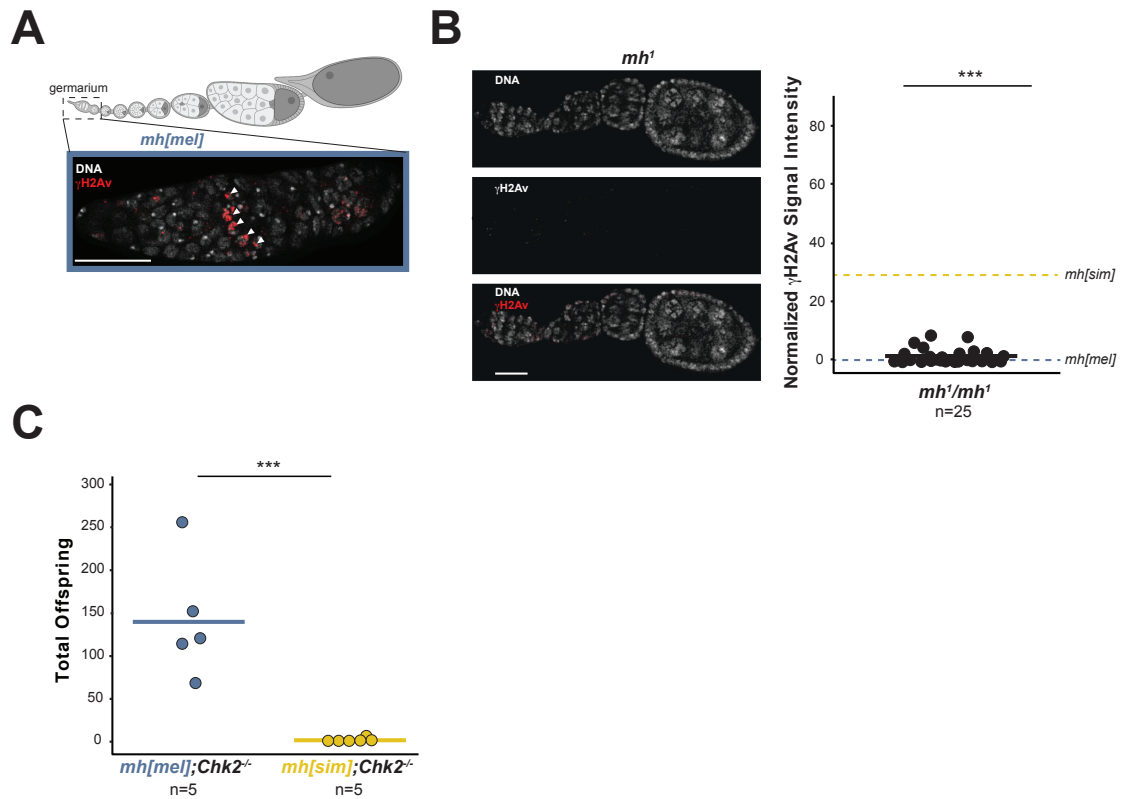
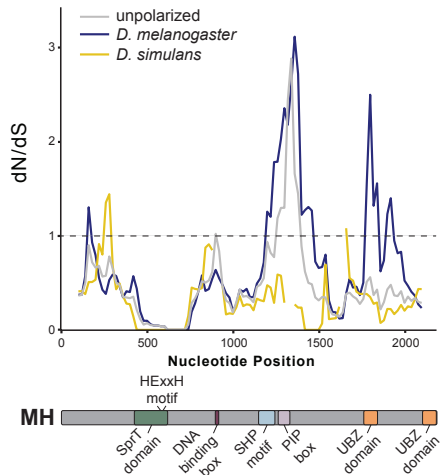


Figure S3. DNA damage signaling further distinguishes MH[sim] from *mh* null. Related to Figure 2. (A) *Drosophila* ovariole (above) showing the germarium where meiotic recombination occurs. Germarium of an *mh[mel]* female (below) showing programmed double-strand breaks (arrowheads) occurring in “region 2A” of the germarium detected under higher laser power relative to images displayed in Figure 2D. These double-strand breaks are repaired via meiotic recombination pathways. (B) γ H2Av signal in *mh¹* ovaries and quantification of normalized fluorescent signal intensity. (C) Progeny counts from *mh[mel]; Chk2^{-/-}* and *mh[sim]; Chk2^{-/-}* females crossed to wildtype (*w¹¹¹⁸*) males. Note that *mh[mel]; Chk2^{-/-}* reduced progeny counts are due to the *Chk2^{-/-}* mutation.^{S1} In panel B, dotted lines correspond to *mh[mel]* and *mh[sim]* averages reported in Figure 2D. (*t*-test: “****” = $p < 0.001$, scale bar = 25 μ m)

A**B**

	Poly-morphism	Fixation
Syn	50	112
Non-syn	8	56

Figure S4. Lineage-specific MH adaptive evolution and Top2 adaptive evolution. Related to Figure 1 and Figure 4. (A) A 200bp sliding window of dN/dS across the *mh* coding region. dN/dS estimates from a comparison of *D. melanogaster* and *D. simulans* are in grey. dN/dS estimates from a comparison of *D. melanogaster* and the *D. melanogaster*-*D. simulans* reconstructed ancestor are in blue. dN/dS estimates from a comparison of *D. simulans* and the *D. melanogaster*-*D. simulans* reconstructed ancestor are in yellow. Windows without synonymous sites are represented as gaps. Windows of dN/dS > 1 are significantly enriched in the *D. melanogaster* lineage (Table S2). (B) Counts of synonymous and nonsynonymous polymorphic and fixed sites within and between *D. melanogaster* and *D. simulans*; χ^2 test, $p = 0.004$.

		Polymorphism	Fixation
Synonymous	<i>D. melanogaster</i> lineage	4	36
	<i>D. simulans</i> lineage	12	17
	Unpolarized	21	65
Non-Synonymous	<i>D. melanogaster</i> lineage	4	48
	<i>D. simulans</i> lineage	8	20
	Unpolarized	12	83

Table S1. Counts of unpolarized and polarized synonymous and non-synonymous polymorphic and fixed sites in the *mh* coding sequence. Related to Figure 1. Unpolarized MK-test: χ^2 , $p = 0.04$. *D. melanogaster* lineage MK-test: χ^2 , $p = 0.70$. *D. simulans* lineage MK-test: χ^2 , $p = 0.31$.

	dN/dS windows < 1	dN/dS windows > 1
<i>D. melanogaster mh</i> – ancestor <i>mh</i>	80	21*
<i>D. simulans mh</i> – ancestor <i>mh</i>	93	3

Table S2. Lineage-specific dN/dS analysis of *mh* in 200bp windows. Related to Figure 1 and Figure S4. *Windows with dN/dS >1 are enriched along the *D. melanogaster* lineage (Fisher's Exact Test, $p = 0.0001$)

Forward	Reverse	Purpose
GATCCAGGAAATACTCGGCC ATCCTGGCCAACAGTGACTC	CCAAAGACTGGTCACACTGC	Primers used to amplify the <i>mh</i> ortholog in <i>D. simulans</i>
	TTTGCCCAAAATATCGAACG	Sequencing primer for <i>mh</i> ortholog in <i>D. simulans</i>
GCAGAGCAGACGAGTCAGTG		Sequencing primer for <i>mh</i> ortholog in <i>D. simulans</i>
	TTGACCTTGTGTGAGGACGA	Sequencing primer for <i>mh</i> ortholog in <i>D. simulans</i>
ACGACGCCTCTTTTTGGTAA		Sequencing primer for <i>mh</i> ortholog in <i>D. simulans</i>
	ACATACGCAACTGGTTCGAC	Sequencing primer for <i>mh</i> ortholog in <i>D. simulans</i>
CACCTTGTTGATCGTCTCCA		Sequencing primer for <i>mh</i> ortholog in <i>D. simulans</i>
	GATCCCACTCCGGACATCTA	Sequencing primer for <i>mh</i> ortholog in <i>D. simulans</i>
TTCTCCATTTTTGTCTTGTGGA		Sequencing primer for <i>mh</i> ortholog in <i>D. simulans</i>
AAGTGTCGCGCTATTTCAACC	TCACCGTCATGGTCTTTGTAGTCCAT	Reverse primer anneals in FLAG-tag. Amplifies <i>mh[mel]</i> and <i>mh[sim]</i> CRISPR-introduced transgenes
AATGGATTTTCGGCAAATGAG	GTCGTTGTAGGAGCCCATGT	Primers anneal outside homology arms. Amplicon spans entire <i>mh[mel]</i> and <i>mh[sim]</i> CRISPR-introduced transgenes
ATGCGCAGGCTAAATTCGAT		Sequencing primer for <i>mh[mel]</i> and <i>mh[sim]</i> region
GATTACCTGTTCGCCCTGAA		Sequencing primer for <i>mh[mel]</i> and <i>mh[sim]</i> region
ACCAACATCACCGTGTACCA		Sequencing primer for <i>mh[mel]</i> and <i>mh[sim]</i> region
CATTGAGCACATCGACCTGT		Sequencing primer for <i>mh[mel]</i> region
CATCGAGAACATCGATATCT		Sequencing primer for <i>mh[sim]</i> region
CTCCCTGACCAGCAAGGAT		Sequencing primer for <i>mh[mel]</i> region
CAGCTTCACCTCCAAGGAT		Sequencing primer for <i>mh[sim]</i> region
TCACGAATTCCGCCCTCT		Sequencing primer for <i>mh[mel]</i> and <i>mh[sim]</i> region
GGCCCTGCTCATATCGTATC	AAGAACCTTACTGCGTGCAAC	Primers anneal in <i>mh</i> introns. Amplifies endogenous <i>mh</i> gene in <i>D. melanogaster</i> .
TATTCTTACATCTATGTGACC	GTTTTGAGCAGCTAATTACC	Primers amplify a repeat unit of the 359-bp satellite array ^{S2}
	CAGGTTTCAGGGCGAACAGGTAATCGGCG	Nested gene specific primer A used for genome walking
	TGATGAACCACCCTTGTATCGTCATCC	Nested gene specific primer B used for genome walking
	TCACCGTCATGGTCTTTGTAGTCCAT	Nested gene specific primer C used for genome walking
TGGGTACAGTGCGCATTTCAT	CGAGCAAGTCCGCAAAAAGT	Primers used to amplify the <i>Top2</i> ortholog in <i>D. simulans</i>
CAGCTTAAGCACAGCGACAC		Sequencing primer for <i>Top2</i> ortholog in <i>D. simulans</i>
CCAGCTTCACCGTTGAGACT		Sequencing primer for <i>Top2</i> ortholog in <i>D. simulans</i>
TAGCTACCTACAAGGGCGGT		Sequencing primer for <i>Top2</i> ortholog in <i>D. simulans</i>
AGGGAGACTCAGCCAAGTCA		Sequencing primer for <i>Top2</i> ortholog in <i>D. simulans</i>
TTTTCAAGACATGCAGCGCC		Sequencing primer for <i>Top2</i> ortholog in <i>D. simulans</i>
GCCAGCGCTCGTTACATTTT		Sequencing primer for <i>Top2</i> ortholog in <i>D. simulans</i>
CCACCGTTCGCTTTGTGATC		Sequencing primer for <i>Top2</i> ortholog in <i>D. simulans</i>
CGATCCGAAAAGGCCTTTA		Sequencing primer for <i>Top2</i> ortholog in <i>D. simulans</i>
AAGCAGATCCTGATGCCAGC		Sequencing primer for <i>Top2</i> ortholog in <i>D. simulans</i>

Table S3. Primers used in this study. Related to STAR Methods.

SUPPLEMENTAL REFERENCES

S1. Xu, J., and Du, W. (2003). *Drosophila* chk2 plays an important role in a mitotic checkpoint in syncytial embryos. *FEBS Lett* 545, 209-212. [10.1016/s0014-5793\(03\)00536-2](https://doi.org/10.1016/s0014-5793(03)00536-2).

S2. Rosic, S., Kohler, F., and Erhardt, S. (2014). Repetitive centromeric satellite RNA is essential for kinetochore formation and cell division. *J Cell Biol* 207, 335-349. [10.1083/jcb.201404097](https://doi.org/10.1083/jcb.201404097).